

EVIDENCE FOR A TRIAXIAL MILKY WAY DARK MATTER HALO FROM THE SAGITTARIUS STELLAR TIDAL STREAM

DAVID R. LAW^{1,2}, STEVEN R. MAJEWSKI³, KATHRYN V. JOHNSTON⁴

DRAFT: August 13, 2018

ABSTRACT

Observations of the lengthy tidal streams produced by the destruction of the Sagittarius dwarf spheroidal (Sgr dSph) are capable of providing strong constraints on the shape of the Galactic gravitational potential. However, previous work, based on modeling different stream properties in axisymmetric Galactic models has yielded conflicting results: while the angular precession of the Sgr leading arm is most consistent with a spherical or slightly oblate halo, the radial velocities of stars in this arm are only reproduced by prolate halo models. We demonstrate that this apparent paradox can be resolved by instead adopting a triaxial potential. Our new Galactic halo model, which simultaneously fits all well-established phase space constraints from the Sgr stream, provides the first conclusive evidence for, and tentative measurement of, triaxiality in an individual dark matter halo. The Milky Way halo within ~ 60 kpc is best characterized by a minor/major axis ratio of the isoveLOCITY contours $c/a \approx 0.67$, intermediate/major axis ratio $b/a \approx 0.83$, and triaxiality parameter $T \sim 0.56$. In this model, the minor axis of the dark halo is coincident with the Galactic X axis connecting the Sun and the Galactic Center to within $\sim 15^\circ$, while the major axis also lies in the Galactic plane, approximately along the Galactic Y axis.

Subject headings: Galaxy: halo — Galaxy: structure — Galaxy: kinematics and dynamics

1. INTRODUCTION

One of the general predictions of structure formation within the prevailing cold dark matter (CDM) paradigm is that galaxy-scale dark matter haloes should be described by a triaxial density ellipsoid (e.g., Jing & Suto 2002; Bailin & Steinmetz 2005; Allgood et al. 2006, and references therein). The characteristic axial ratios of these haloes are typically expected to be far from spherical (see, e.g., Bullock et al. 2002; Kuhlen et al. 2007; and references therein) with characteristic central minor/major axis ratios (in the isoveLOCITY contours) $c/a \sim 0.72$ and intermediate/major axis ratios $b/a \sim 0.78$ (Hayashi et al. 2007). Adopting the triaxiality parameter of Franx et al. (1991),

$$T = \frac{1 - b^2/a^2}{1 - c^2/a^2} \quad (1)$$

this corresponds to a typical value of $T = 0.81$. As discussed by Hayashi et al. (2007), there can be significant variation of the axis ratios with radius and between realizations of similar mass haloes: individual values for c/a range from $\sim 0.6 - 0.9$ while b/a can take values $\sim 0.6 - 1.0$. Despite the near-ubiquitous predictions of triaxiality from such simulations, there has hitherto been little observational evidence to confirm triaxiality in specific individual galaxies: while gravitational lensing (e.g., Hoekstra et al. 2004; Mandelbaum et al. 2006; Evans et al. 2009) and X-ray observations (e.g., Pointecouteau et al. 2005) have indicated that non-sphericity appears to

be common in dark matter haloes, such studies are sensitive only to the integral of the density profile along the line of sight and do not provide fully 3-D information.

The Milky Way Galaxy provides perhaps the best laboratory for testing predictions of halo sphericity since the tidal stream remnants of dwarf satellites orbiting in the Galactic halo can be traced in three dimensions and provide sensitive probes of the underlying mass distribution. The tidal tails emanating from the Sagittarius dwarf spheroidal galaxy (Sgr dSph)⁵ have been used for such efforts since shortly after the discovery of the dwarf by Ibata et al. (1994). Early efforts to model the MW — Sgr system (e.g., Johnston et al. 1995, 1999; Velazquez & White 1995; Edelson & Elmegreen 1997; Ibata et al. 1997; Gómez-Flechoso et al. 1999; Helmi & White 2001) generally concentrated on fitting the orbit of Sgr within an adopted Milky Way potential. In more recent years however, compelling wide-field views of the extensive tidal streams associated with the dwarf have been provided by the Two Micron All-Sky Survey (2MASS; Majewski et al. 2003) and Sloan Digital Sky Survey (SDSS; Belokorov et al. 2006), and permitted much more detailed exploration of the underlying shape of the Galactic potential to be undertaken by Helmi (2004), Martínez-Delgado et al. (2004, 2007), Law, Johnston, & Majewski (2005; hereafter LJM05), Fellhauer et al. (2006), and Cole et al. (2008). Despite the prediction from CDM theory that the Milky Way should be best described by a triaxial Galactic potential, the majority of models to date (although cf. Gnedin et al. 2005) have adopted an axisymmetric framework in which flattening is introduced only into the Galactic Z axis (i.e. perpendicular to the Galactic disk).

⁵ We refer the non-expert reader to LJM05 (see particularly their Fig. 1) for an extended introduction to the general characteristics of the Sgr dwarf system.

¹ Hubble Fellow.

² Department of Physics and Astronomy, University of California, Los Angeles, CA 90095; drlaw@astro.ucla.edu

³ Dept. of Astronomy, University of Virginia, Charlottesville, VA 22904-0818 (srm4n@virginia.edu)

⁴ Department of Astronomy, Columbia University, New York, NY 10027 (kvj@astro.columbia.edu)

While these recent simulations agree on many aspects of the Sgr orbit, no one model has yet been capable of reproducing all of the observational data and these models reach different conclusions about the shape of the Galactic halo depending on which observational data are weighted as primary constraints: Some studies favor a mildly oblate halo (e.g., Johnston et al. 2005 [hereafter JLM05]; Martínez-Delgado et al. 2007), some an approximately spherical halo (e.g., Ibata et al. 2001; Fellhauer et al. 2006), and others a prolate halo (e.g., Helmi 2004). The crux of this “halo conundrum” (highlighted by JLM05, and also discussed by Fellhauer et al. 2006, Martínez-Delgado et al. 2007, Newberg et al. 2007, and Yanny et al. 2009) is that in an axisymmetric Galactic potential it is not possible to simultaneously fit both the angular precession and distance/apparent radial velocity of stars in the leading Sgr stream as it arcs through the North Galactic Cap towards the Galactic anticenter. In order to match the angular coordinates of stars in the Sgr leading arm JLM05 and Fellhauer et al. (2006) required mildly oblate or nearly spherical models (with Z -axis flattening $q_z \sim 0.9 - 1.05$ in the contours of the gravitational potential) for the Galactic dark halo. Such models cause the leading arm to reenter the Galactic disk in the vicinity of the Sun (to within $\sim 5 - 10$ kpc), in contradiction with photometric distance estimates (e.g., Newberg et al. 2007) from SDSS. Such a model also predicts a significant projection of the orbital velocities of leading tidal debris onto the observed line of sight, in contrast to spectroscopic radial velocity data (presented by Law et al. 2004, LJM05, and more recently confirmed by Yanny et al. 2009). In order to reproduce the radial velocity and distance trends the halo must be prolate with $q_z \sim 1.25$ (as demonstrated by Helmi et al. 2004 and confirmed by LJM05), but this in turn cannot account for the observed precession experienced by the tidal debris.

In this Letter we demonstrate that this “halo conundrum” is a consequence of the near-ubiquitous adoption of axisymmetric models for the Galactic potential. By using fully triaxial models, similar to those predicted by standard CDM theory, it is possible to simultaneously satisfy all constraints imposed by the structure of Sgr debris on the Milky Way’s mass distribution.

2. MODEL

We adopt a basic formalism similar to that described by LJM05 (and described in greater detail by Law et al., *in prep.*) in which the Milky Way is described by a smooth fixed gravitational potential consisting of a Miyamoto-Nagai (1975) disk, Hernquist spheroid, and a logarithmic halo. The respective contribution of these components to the gravitational potential is given by:

$$\Phi_{\text{disk}} = -\alpha \frac{GM_{\text{disk}}}{\sqrt{R^2 + (a + \sqrt{z^2 + b^2})^2}}, \quad (2)$$

$$\Phi_{\text{sphere}} = -\frac{GM_{\text{sphere}}}{r + c}, \quad (3)$$

$$\Phi_{\text{halo}} = v_{\text{halo}}^2 \ln(C_1 x^2 + C_2 y^2 + C_3 xy + (z/q_z)^2 + r_{\text{halo}}^2) \quad (4)$$

where the various constants C_1 , C_2 , C_3 are given by

$$C_1 = \left(\frac{\cos^2 \phi}{q_1^2} + \frac{\sin^2 \phi}{q_2^2} \right) \quad (5)$$

$$C_2 = \left(\frac{\cos^2 \phi}{q_2^2} + \frac{\sin^2 \phi}{q_1^2} \right) \quad (6)$$

$$C_3 = 2 \sin \phi \cos \phi \left(\frac{1}{q_1^2} - \frac{1}{q_2^2} \right) \quad (7)$$

This form for the halo potential permits flattening to be introduced along the three axes q_1 , q_2 , q_z , where q_z represents the flattening perpendicular to the Galactic Plane, while q_1 and q_2 are free to rotate in the Galactic Plane at an angle ϕ to a right-handed Galactocentric X, Y coordinate system⁶. Since it is only the *ratios* between these q that have physical significance, we fix $q_2 = 1.0$ and explore the effects of varying q_1 and q_z in the range $1.0 - 1.8$, with $\phi = 0^\circ - 180^\circ$. We do not consider the range $q_z, q_1 > 1.8$ since our formulation of the Galactic gravitational potential rapidly becomes unphysical for larger values.

We note that this method introduces the flattening directly into the gravitational potential (i.e. the isovelocity contours) for ease of calculation and consistency with previous studies (e.g., LJM05). We have also considered more physical models in which axial flattenings are introduced into the density profile of an NFW (Navarro et al. 1996) halo model, and the resulting accelerations computed using the approximate form of the potential given by Lee & Suto (2003). Such models give slightly different orbital paths, but the qualitative results discussed below remain essentially unchanged.

We assume that the Sun is located 8.0 kpc from the Galactic Center and 28 kpc from the Sgr core (Siegel et al. 2007). We fix various constants in Equations 2 - 4 based on previous work by LJM05, adopting $M_{\text{disk}} = 1.0 \times 10^{11} M_\odot$, $M_{\text{sphere}} = 3.4 \times 10^{10} M_\odot$, $a = 6.5$ kpc, $b = 0.26$ kpc, $c = 0.7$ kpc, $r_{\text{halo}} = 12$ kpc. Similarly, the position, radial velocity, and instantaneous orbital plane of the Sgr dwarf are fixed as discussed in LJM05 (see also Law et al., *in prep.*).

For each combination of q_1 , q_z , and ϕ tested we proceed as follows; (1) We fixed v_{halo} in Equation 4 so that the LSR has an orbital velocity $v_{\text{LSR}} = 220 \text{ km s}^{-1}$. (2) While the dynamics of the *leading* arm of Sgr tidal debris are strongly dependent on the choice of Galactic potential, the *trailing* arm experiences very little precession and its characteristic angular position (Majewski et al. 2003) and radial velocities (Majewski et al. 2004) can be well reproduced in any realistic model of the Galactic potential given suitable choice of the speed v_{tan} of Sgr perpendicular to the line of sight (as demonstrated by LJM05). We therefore adjusted v_{tan} until the best match to the trailing debris data was obtained. (3) Massless test-particles were integrated along the orbit, and the quality of fit χ to the observational data calculated.

The accuracy of such test-particle orbits will necessarily be limited since actual tidal debris (with a range of orbital energies and angular momenta) from massive satellites will deviate slightly from these orbits; leading/trailing arms will fall inside/outside the orbital path respectively (see, e.g., discussion by Johnston et al. 1995, 1999; Choi et al. 2007; Eyre & Binney 2009). However,

⁶ I.e., when $\phi = 0^\circ$, q_1 is aligned with the Galactic X axis and Eqn. 4 reduces to $\Phi_{\text{halo}} = v_{\text{halo}}^2 \ln([x/q_1]^2 + [y/q_2]^2 + [z/q_z]^2 + r_{\text{halo}}^2)$.

previous work (e.g., LJM05) has demonstrated that for Sgr the test-particle orbits provide a good indication of the general trend of tidal debris (particularly for the observational constraints upon which we focus) and suffice for the first-order estimate of the underlying gravitational potential presented here.

3. RESULTS

We first illustrate the spirit of our results with the specific case of $\phi = 90^\circ$ (i.e. $q_1 = q_y$). In Figure 1 we plot radial velocity (with respect to the Galactic Standard of Rest [GSR]) and declination along the section of orbit leading the Sgr dwarf for models in which the Milky Way is taken to have various values of q_y and q_z . While the trend of radial velocity is strongly affected by the choice of q_z (i.e. different colors in upper panels of Fig. 1), q_y has a comparatively minor effect on the velocities (difference between solid/dotted/dashed lines of a given color) in the key range $\alpha \sim 250^\circ - 100^\circ$. In contrast, both q_y and q_z affect the precession of the leading arm as characterized by its declination δ for a given α or Λ_\odot coordinate. As shown in the lower panels of Figure 1, increasing q_z shifts the arm to greater δ for fixed q_y (i.e. changing from black, to orange, to magenta curves for a given line type in Fig. 1), and increasing q_y decreases δ for fixed q_z (i.e. changing from solid, to dotted, to dashed curves for a given line color in Fig. 1). These trends indicate that while both q_y and q_z govern the angular precession of the stream, it is primarily q_z that affects the distance to the leading arm, altering the projection of the orbital velocity onto the line of sight.

In the special case of $\phi = 90^\circ$, q_z and q_1 are clearly separable parameters which may be constrained in turn. In general however, q_z and q_1 are not separable and must be constrained in tandem so that the resulting tidal stream matches both the apparent radial velocity and the observed angular precession. In Figure 2 we summarize the three most relevant observational constraints: trailing arm velocity data from Majewski et al. (2004; open circles), leading arm angular coordinates from Belokurov et al. (2006; open triangles), and leading arm radial velocities from Law et al. (2004; see also LJM05 and Majewski et al. *in prep.*; open boxes). While there is evidence for a ‘‘bifurcation’’ in the Sgr leading stream (Belokurov et al. 2006), we assume that the centroid of the stream is represented by the main, highest surface-brightness ‘southern’ branch (see discussion by Yanny et al. 2009; Law et al. *in prep.*). As discussed in §2, it is possible to fit the trailing arm velocity data in most reasonable models of the Galactic potential with suitable choice of the velocity of Sgr along its orbit, and all of our models are designed to do so.

We define a χ^2 statistic characterizing the quality of fit of the Sgr orbit in our various models of the Galactic halo to the angular coordinates and velocity data:

$$\begin{aligned} \chi^2 = & \frac{1}{n_{v,\text{lead}} - 3} \sum_i \frac{(v_{\text{orbit}}[i] - v_{\text{obs,lead}}[i])^2}{\sigma_v^2} \\ & + \frac{1}{n_{v,\text{trail}} - 3} \sum_i \frac{(v_{\text{orbit}}[i] - v_{\text{obs,trail}}[i])^2}{\sigma_v^2} \\ & + \frac{1}{n_\delta - 3} \sum_i \frac{(\delta_{\text{orbit}}[i] - \delta_{\text{obs}}[i])^2}{\sigma_\delta^2} \end{aligned} \quad (8)$$

where $n_{v,\text{lead}} = 94$, $n_{v,\text{trail}} = 108$, and $n_\delta = 17$, the number of observational data points in the 2MASS leading/trailing radial velocity samples and the SDSS survey fields along the main branch of the Sgr stream respectively. We adopt an uncertainty $\sigma_v = 12\text{km s}^{-1}$ for each radial velocity measurement (this represents a combination of observational uncertainty and intrinsic stream width; see discussion in Majewski et al. 2004), and $\sigma_\delta = 1.9^\circ$ for each survey field location from Belokurov et al. (2006)⁷. The radial velocity v_{orbit} and angular location δ_{orbit} of the orbit at each longitudinal position ($\Lambda[i]$ or $\alpha[i]$ respectively) is determined via linear interpolation of the orbital path.

In Figure 3 we show the values of χ resulting from various choices for ϕ , q_1 , and q_z . Values of $\phi \approx 90^\circ - 105^\circ$ (i.e. q_1 nearly aligned with the Galactic Y axis) are strongly favored and are the only models in which values of $\chi < 5$ can be obtained. Given the limitations of the orbit-fitting method, it is not possible to conclusively discriminate between q_1 - q_z pairs in the triaxial region of parameter space $q_z \approx 1.2 - 1.4$ (green/cyan/blue lines respectively in Fig. 3) and $q_1 \approx 1.2 - 1.8$ since deviations of the actual tidal debris from the orbital path of the bound satellite are expected to have an effect comparable in magnitude to the computed values of $\chi \approx 3$. More detailed fitting incorporating finer sampling scales in q_z , q_1 , and ϕ in combination with comprehensive N-body models is beyond the scope of the present work and will be presented by Law et al. (*in prep.*); at present we note simply that the absolute minimum ($\chi = 2.7$) occurs for $\phi = 90^\circ$, $q_z = 1.25$, $q_1 = q_y = 1.5$. The Laplacian of this potential is everywhere positive, indicating that it corresponds to a physically realizable density distribution.

4. DISCUSSION

In LJM05 we conducted an extensive parameter space search exploring the effects of varying the Galactic disk/bulge mass, the dark halo scale length, Sgr kinematics, the distance to the Galactic Center, the distance to Sgr, and the total mass scale of the Milky Way. No variation of these parameters gave rise to a model in which it was possible to simultaneously reproduce all three observational constraints (trailing velocities, leading precession, leading velocities) on the Sgr stream in an axisymmetric Galactic halo. In Figure 2 we overplot on the observational constraints the orbits in an axisymmetric halo that best fit individual constraints: the black curve is chosen to best-fit the angular precession of the leading arm ($q_1 = 1.00$, $q_z = 0.97$), while the green curve is chosen to best fit the radial velocity trend of the leading arm ($q_1 = 1.00$, $q_z = 1.25$). These models have quality-of-fit parameters $\chi = 8.3/9.4$ respectively. In contrast, the red curve in Figure 2 represents our best-fit orbit in a triaxial halo with $q_z = 1.25$, $q_1 = 1.50$, $\phi = 90^\circ$: in this model the orbit of the Sgr dwarf simultaneously reproduces both the observed run of angular precession and radial velocity for the leading arm. The corresponding ratios for the minor/major ($c/a = 0.67$) and intermediate/major ($b/a = 0.83$) axis ratios in this triaxial halo are broadly consistent with the typical values predicted

⁷ This uncertainty is a rough estimate of the uncertainty in the centroid of the stream at a given longitude based on the apparent width of the stream.

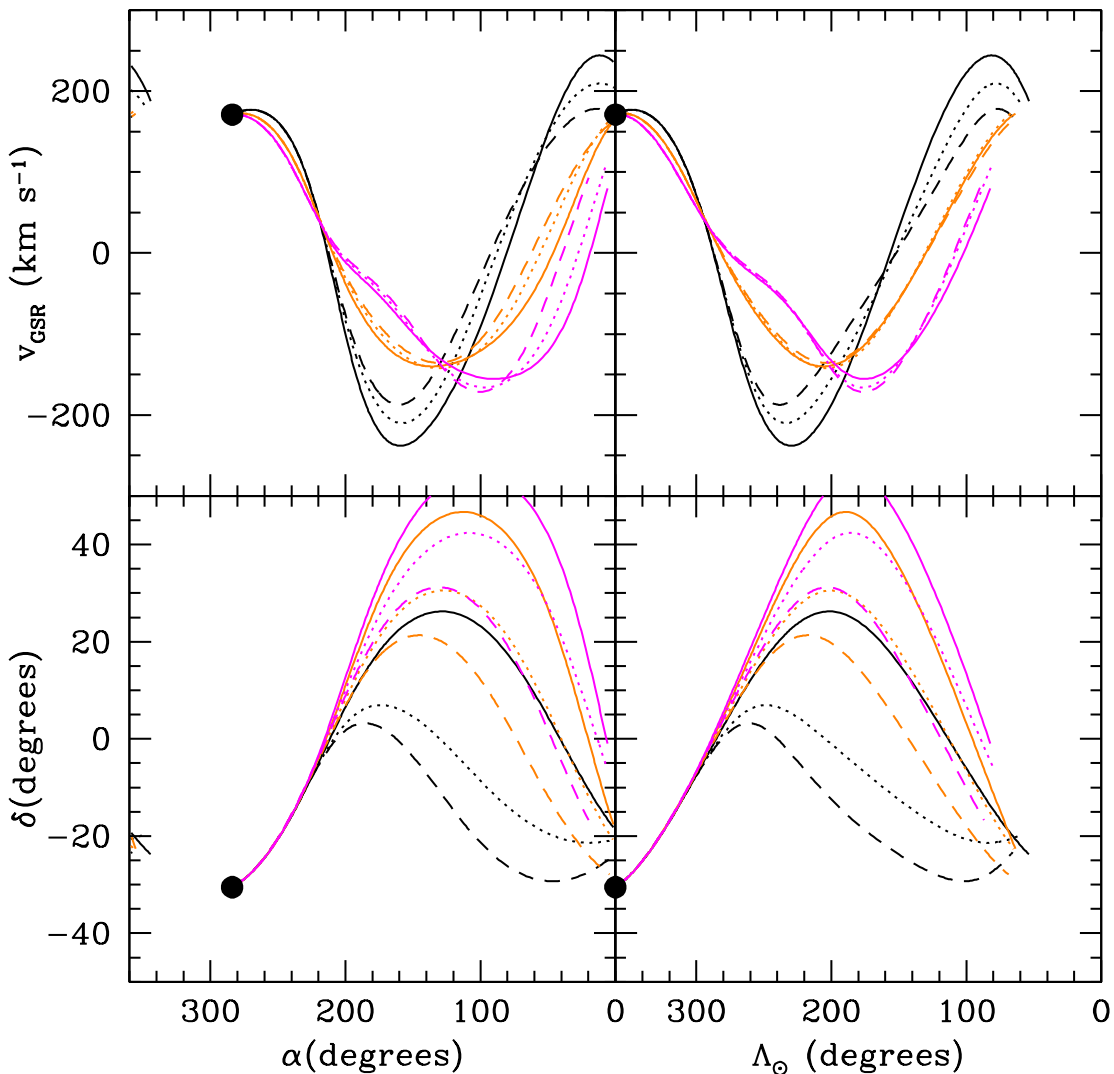


FIG. 1.— Model orbits are plotted 1.2 Gyr in advance of the current position of the Sgr dwarf (denoted by filled circles) illustrating the trend of declination (δ ; bottom panels) and apparent radial velocity (v_{GSR} ; top panels) expected for leading arm tidal debris. Black/orange/magenta curves respectively denote haloes in which $q_z = 1.0/1.3/1.6$ while solid/dotted/dashed curves correspond to values $q_y = 1.0/1.3/1.6$ (i.e. $\phi = 90^\circ$) respectively. Given the split in the literature between describing position along the orbit in terms of the right ascension (α) or the more natural orbital longitude (Λ_\odot ; see Majewski et al. 2003) we show these relations against both α and Λ_\odot in left/right-hand panels respectively to aid comparison to plots published by previous authors.

by cosmological simulations (e.g., Hayashi et al. 2007), although the best-fit triaxiality parameter $T \approx 0.56$ is somewhat lower than anticipated.

While the fit may change somewhat with detailed N-body models, we can conclude not only that the Galactic dark halo may be triaxial within the orbit of Sgr ($r \lesssim 60$ kpc), but that the short/long axes of the halo may be aligned with the Galactic X/Y axes respectively to within $\sim 15^\circ$. If the axial flattenings are introduced into an NFW model of the dark matter density distribution, qualitatively similar results are obtained with $q_{\rho,x}/q_{\rho,y}/q_{\rho,z} = 1.0/2.0/1.66$. As expected (e.g., Kuhlen et al. 2007) the isoveLOCITY contours are more spherical than the isodensity contours, but both indicate a similar preference for a triaxial system in which the major/minor axes are approximately aligned with the Galactic Y/X

axes respectively.

This alignment is somewhat similar to that of the *stellar* halo described by Newberg & Yanny (2006), who found a major axis similarly aligned with the Galactic Y axis to within $\sim 20 - 40^\circ$, albeit with a minor axis along Z rather than X. There is no clear correlation however with the triaxiality of the Galactic bulge: the long axis of the bar is currently thought to lie within $\sim 15 - 20^\circ$ of the Galactic X axis (e.g., Nakada et al. 1991; Morris & Serabyn 1996; Babusiaux & Gilmore 2005), close to the minor axis of the dark halo.

In closing, we note two complications of the above results. First, our analysis has assumed that the disk lies in one of the symmetry planes of the halo potential and that the axes themselves do not twist with radius. While such assumptions should be explored with future studies,

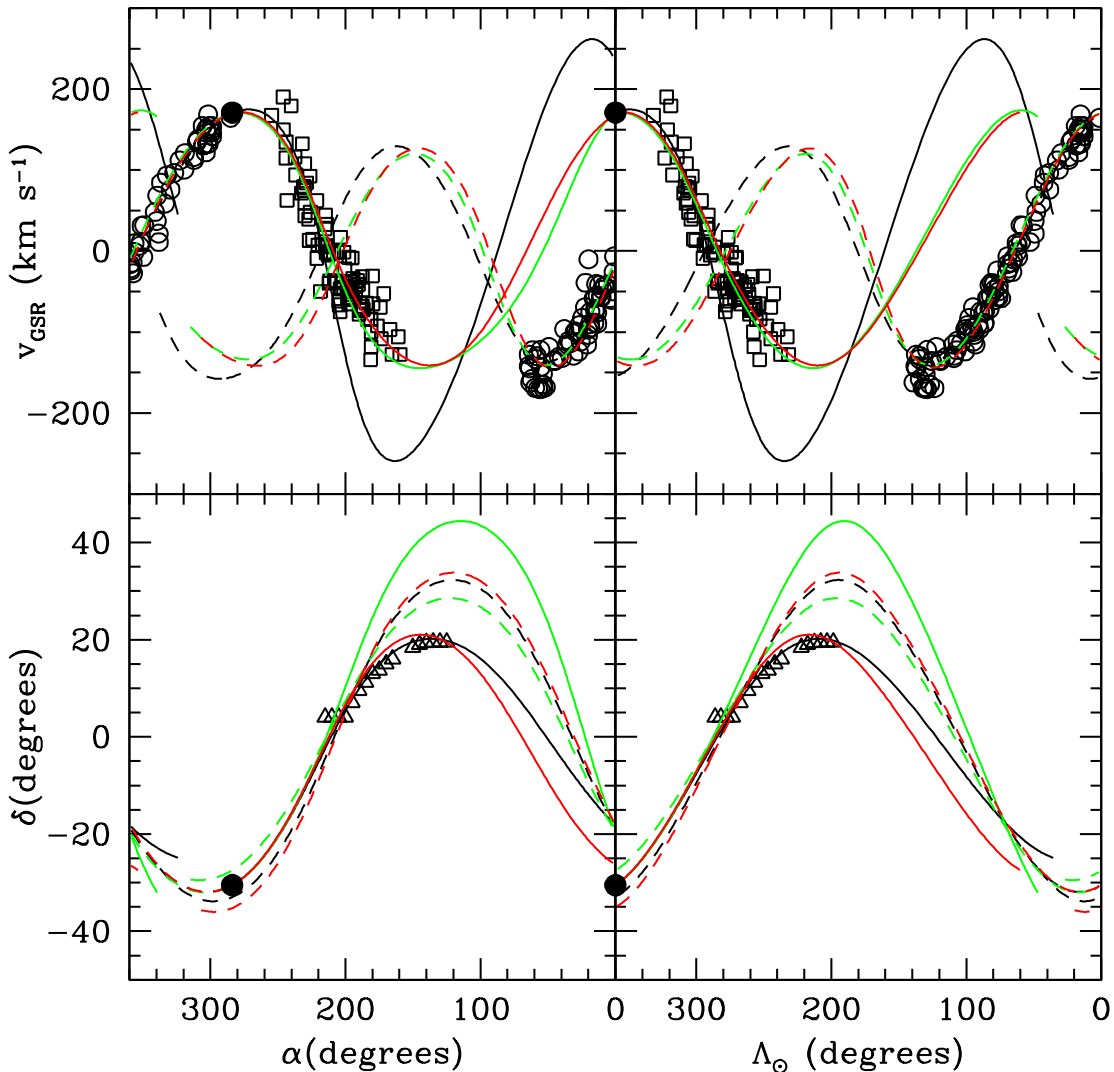


FIG. 2.— Model orbits are plotted for three models: Axisymmetric halo best fitting leading arm precession (black curve), axisymmetric halo best fitting leading arm velocities (green curve), and triaxial halo model (red curve). Solid/dashed lines indicate the orbital path of Sgr leading/trailing its current position for 1.2 Gyr. Open triangles represent SDSS data from Belokorov et al. (2006), open squares/circles represent leading/trailing arm M-giant radial velocity data from Law et al. (2004) and Majewski et al. (2004) respectively. Note that although the solid black curve fits the angular coordinates well it provides a poor match to the radial velocities; the solid green curve provides a good match to the radial velocities but a poor match to the angular coordinates; but the red curve matches both velocities and angular coordinates well.

we do not expect the broad results of our study to change — an orientation significantly out of a symmetry plane would result in warping of the disk, which would dampen the misalignment on timescales of a few disk orbits (e.g., Dubinski & Kuijken 1995; Bailin et al. 2007; Jeon et al. 2009). Second, in the family of models presented here the Galactic Z axis is the intermediate axis of the triaxial ellipsoid. In a global sense such models are somewhat unsatisfactory since orbits about this axis (i.e. in the plane of the Galactic disk) are expected to be unstable (e.g., Binney et al. 1981). At present, however, such

models are the only ones in which it is possible to simultaneously reproduce all of the observed characteristics of the Sgr stream.

Support for this work was provided by NASA through Hubble Fellowship grant # HF-01221.01 awarded by the Space Telescope Science Institute, which is operated by the Association of Universities for Research in Astronomy, Inc., for NASA, under contract NAS 5-26555. SRM acknowledges support from National Science Foundation grant AST-0807945.

REFERENCES

Allgood, B., Flores, R. A., Primack, J. R., Kravtsov, A. V., Wechsler, R. H., Faltenbacher, A., & Bullock, J. S. 2006, MNRAS, 367, 1781

Babusiaux, C., & Gilmore, G. 2005, MNRAS, 358, 1309

Bailin, J., & Steinmetz, M. 2005, ApJ, 627, 647

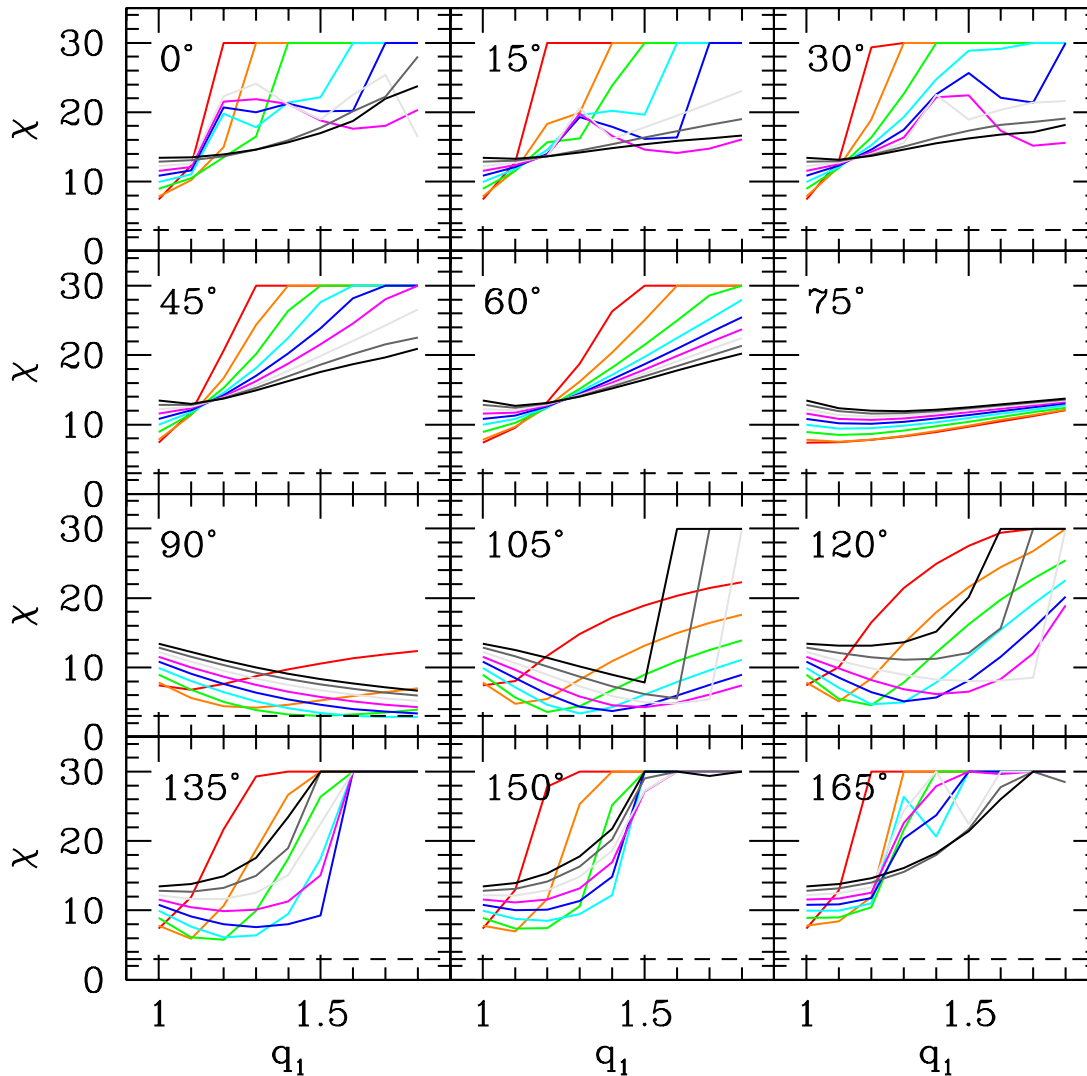


FIG. 3.— Quality-of-fit parameter χ is shown as a function of the axial flattening q_1 in the Galactic Plane for various choices of the axial rotation angle (ϕ) and the flattening perpendicular to the Galactic Plane (q_z). Numbers in each panel represent the value of ϕ , while red/orange/green/cyan/blue/magenta/light grey/dark grey/black curves respectively correspond to $q_z = 1.0/1.1/1.2/1.3/1.4/1.5/1.6/1.7/1.8$. The dashed line represents $\chi = 3.0$, curves approach this line only for $\phi \sim 90^\circ - 105^\circ$. Note that $\phi = 0^\circ$ corresponds to q_1 lying along the Galactic X axis, and $\phi = 90^\circ$ to the Galactic Y axis.

Bailin, J., Simon, J. D., Bolatto, A. D., Gibson, B. K., & Power, C. 2007, *ApJ*, 667, 191
 Belokurov, V., et al. 2006, *ApJ*, 642, L137
 Binney, J. 1981, *MNRAS*, 196, 455
 Bullock, J. S. 2002, *The Shapes of Galaxies and their Dark*, 109
 Choi, J.-H., Weinberg, M. D., & Katz, N. 2007, *MNRAS*, 381, 987
 Cole, N., et al. 2008, *ApJ*, 683, 750
 Dubinski, J., & Kuijken, K. 1995, *ApJ*, 442, 492
 Edelson, D. J., & Elmegreen, B. G. 1997, *MNRAS*, 290, 7
 Evans, A. K. D., & Bridle, S. 2009, *ApJ*, 695, 1446
 Eyre, A., & Binney, J. 2009, arXiv:0907.0360
 Fellhauer, M., et al. 2006, *ApJ*, 651, 167
 Franx, M., Illingworth, G., & de Zeeuw, T. 1991, *ApJ*, 383, 112
 Gnedin, O. Y., Gould, A., Miralda-Escudé, J., & Zentner, A. R. 2005, *ApJ*, 634, 344
 Gómez-Flechoso, M. A., Fux, R., & Martinet, L. 1999, *A&A*, 347, 77
 Hayashi, E., Navarro, J. F., & Springel, V. 2007, *MNRAS*, 377, 50
 Helmi, A. 2004, *ApJ*, 610, L97
 Helmi, A., & White, S. D. M. 2001, *MNRAS*, 323, 529

Hoekstra, H., Yee, H. K. C., & Gladders, M. D. 2004, *ApJ*, 606, 67
 Ibata, R. A., Gilmore, G., & Irwin, M. J. 1994, *Nature*, 370, 194
 Ibata, R. A., Wyse, R. F. G., Gilmore, G., Irwin, M. J., & Suntzeff, N. B. 1997, *AJ*, 113, 634
 Ibata, R., Lewis, G. F., Irwin, M., Totten, E., & Quinn, T. 2001, *ApJ*, 551, 294
 Jeon, M., Kim, S. S., & Ann, H. B. 2009, *ApJ*, 696, 1899
 Jing, Y. P., & Suto, Y. 2002, *ApJ*, 574, 538
 Johnston, K. V., Spergel, D. N., & Hernquist, L. 1995, *ApJ*, 451, 598
 Johnston, K. V., Majewski, S. R., Siegel, M. H., Reid, I. N., & Kunkel, W. E. 1999, *AJ*, 118, 1719
 Johnston, K. V., Law, D. R., & Majewski, S. R. 2005, *ApJ*, 619, 800
 Kuhlen, M., Diemand, J., & Madau, P. 2007, *ApJ*, 671, 1135
 Law, D. R., Majewski, S. R., Skrutskie, M. F., & Johnston, K. V. 2004, *Satellites and Tidal Streams*, 327, 239
 Law, D. R., Johnston, K. V., & Majewski, S. R. 2005, *ApJ*, 619, 807 (LJM05)
 Lee, J., & Suto, Y. 2003, *ApJ*, 585, 151

- Majewski, S. R., et al. 2004, *AJ*, 128, 245
- Majewski, S. R., Skrutskie, M. F., Weinberg, M. D., & Ostheimer, J. C. 2003, *ApJ*, 599, 1082
- Mandelbaum, R., Hirata, C. M., Broderick, T., Seljak, U., & Brinkmann, J. 2006, *MNRAS*, 370, 1008
- Martínez-Delgado, D., Peñarrubia, J., Jurić, M., Alfaro, E. J., & Ivezić, Z. 2007, *ApJ*, 660, 1264
- Martínez-Delgado, D., Gómez-Flechoso, M. Á., Aparicio, A., & Carrera, R. 2004, *ApJ*, 601, 242
- Miyamoto, M., & Nagai, R. 1975, *PASJ*, 27, 533
- Morris, M., & Serabyn, E. 1996, *ARA&A*, 34, 645
- Nakada, Y., Onaka, T., Yamamura, I., Deguchi, S., Hashimoto, O., Izumiura, H., & Sekiguchi, K. 1991, *Nature*, 353, 140
- Navarro, J. F., Frenk, C. S., & White, S. D. M. 1996, *ApJ*, 462, 563
- Newberg, H. J., Yanny, B., Cole, N., Beers, T. C., Re Fiorentin, P., Schneider, D. P., & Wilhelm, R. 2007, *ApJ*, 668, 221
- Newberg, H. J., & Yanny, B. 2006, *Journal of Physics Conference Series*, 47, 195
- Pointecouteau, E., & Silk, J. 2005, *MNRAS*, 364, 654
- Siegel, M. H., et al. 2007, *ApJ*, 667, L57
- Velazquez, H., & White, S. D. M. 1995, *MNRAS*, 275, L23
- Xu, Y., Deng, L. C., & Hu, J. Y. 2006, *MNRAS*, 368, 1811
- Yanny, B., et al. 2009, *arXiv:0905.4502*